

# Mechanical Studies of Subperiosteal Implants

Klaudia Kulcsar<sup>1,2</sup>, Ibolya Zsoldos<sup>1\*</sup>

<sup>1</sup> Department of Materials Science and Technology, Széchenyi István University, Egyetem sqr 1., H-9026 Győr, Hungary

<sup>2</sup> Dent-Art Technik Ltd., Csokonai u. 10., H-9024 Győr, Hungary

\* Corresponding author, e-mail: [zsoldos@sze.hu](mailto:zsoldos@sze.hu)

Received: 25 October 2023, Accepted: 28 November 2023, Published online: 17 January 2024

## Abstract

When designing subperiosteal implants, mechanical testing of the implant and abutment is inevitable. Subperiosteal implants and their abutments are medical devices made to order, so each implant requires a separate design, since each patient has a different bone surface, for which the implant must be designed. For the mechanical testing of subperiosteal implants, a new test apparatus was constructed, on which mechanical simulations were carried out, the subperiosteal implants were tested together with their abutments. In addition to the finite element analysis simulation, the test apparatus can also be used to determine how much force is generated by the chewing force on the subperiosteal implant and its abutment as a result of the chewing mechanism.

## Keywords

dental implant, titanium alloy, additive technology, mechanical study, mechanical testing equipment

## 1 Introduction

Human masticatory organ is a complex anatomical structure made up of bones, teeth, muscles, tendons, and ligaments. Several different muscles take part in moving the lower jaw, i.e., the mandible. Musculus masseter (masseter muscle), musculus temporalis (temporal muscle) and musculus pterygoideus lateralis (lateral pterygoid) are responsible for elevating the mandible thus closing the jaw. Although, in terms of their exact function each muscle has a dedicated role as well. Musculus masseter is also responsible for the ipsilateral movement of the mandible and partially responsible for its anteroposterior movement as well. Musculus temporalis is made up of an anterior, a medial, and a posterior muscle bundle to create a fan-shaped structure. All three muscle parts are capable of creating a differently-oriented force. The anterior bundle mostly takes part in movements until closing the teeth, while posterior bundles are mainly responsible for connecting the temporomandibular joint surfaces and for pulling back the mandible. Apart from moving the mandible up and down, musculus pterygoideus medialis also plays a key role in moving the mandible both forward and in contralateral directions. Musculus digastricus is responsible for opening the mouth and elevating the hyoid bone during mastication [1]. These muscles not only move the mandible, but also provide stability against asymmetric forces that

emerge during chewing. Connected tendons and ligaments only take part passively in the process of mastication. They only block the dislocation of the jaw in the extreme positions of the temporomandibular joint [2]. It is evident that the jaw is a system capable of one of the most complex movements in the human body. Dynamic modelling of its movements requires much more advanced techniques than knee or hip joints, which also have high importance in the medical device field. In contrast to them, modelling the temporomandibular joint as a simple joint or ball-and-socket joint represents a significant simplification of real biological movements. In addition, articular surfaces of the temporomandibular joint move freely relative to each other during chewing, which further complicates modelling [2]. We can find measurement results on the magnitude of load forces occurring during chewing in previous studies. Ahlgren and Örwall defined average chewing force of males and females between 45-136 N from chewing gum measurements [3]. Examining different types of food, Anusavice provides guidance on the magnitude of the maximum load forces per tooth: they registered 830 N in the molar region; 445 N in the premolar region; 334 N for canine teeth; 111 N for incisors [4]. Test equipment with a chewing function that imitates the movement of the human jaw appear in various areas of use.

Robots with human-machine interaction are described in the literature, with the aim of rehabilitating patients who suffer from insufficiency of the temporomandibular joint, masticatory muscles, or other related organs [5]. Alemzadeh et al. tested an apparatus that imitated chewing a chewing gum to examine drug release from the gum [6]. Modelling the mechanical loads during chewing also plays a significant role in medical device practice involving dental implants and their abutment systems. Here we can mention testing of screw-type implants or subperiosteal implants of complex geometries, and wear testing of crowns and bridges [7]. Raabe et al. assembled a Stewart platform type apparatus with six prismatic actuators for the wear testing of total dentition, crowns, and bridges. The apparatus utilized force and position control [8]. There is no current standard available for the mechanical performance testing of subperiosteal implants. In present practice, mechanical testing of subperiosteal implants is either carried out with custom apparatus or finite element analysis (FEA). Negrini studied Ti-6Al-4V ELI subperiosteal implants manufactured with LPBF (Laser Powder Bed Fusion) additive technology. Experiments on implants were conducted with both finite element method and custom testing apparatus [9]. He validated results of finite element modelling with real-life mechanical testing results. Although, the mechanical testing apparatus majorly simplified anatomical loads. Surface of the subperiosteal implant fitting the bone was joined to an anatomically precise additively manufactured polymer piece, while the abutment was loaded with a simple compression block that could translate along the vertical axis. Instead of loading the abutment components of the implant, its abutments were loaded with a separate ball head geometry to achieve better load distribution [9]. Several studies emerged from finite element analysis of subperiosteal implants. These computer simulations typically included static loading of implants with vertical and oblique forces [10, 11]. Finite element analyses in software environment can be validated with real-world mechanical tests using artificial materials (e.g., bone blocks), with in vivo tests or even with secondary clinical data. At the same time, such validation of finite element modelling involving dental implants is extremely rare in scientific literature. In their literature review looking back from 2018, Chang et al. found a total of 47 studies where the results of finite element modelling on dental implants were subjected to some form of validation. This was less than 10% of all analysed FEA studies. And even from

these 47 studies, none was in connection with subperiosteal implants [12]. Furthermore, among those studies where the results of the finite element models were compared with real mechanical tests, the inaccuracies of the finite element modelling were also shown. Cepic et al. [13], for example, investigated the displacement of the bone – screw implant – abutment under mechanical loads in the case of dentures fixed with screw implants using finite element simulation, which was validated with cadaver tests. Although software modelling results showed similar trends with real-life tests, stiffness of the implant assembly was always underestimated by the model [13].

## 2 Testing apparatus setup

Fig. 1 shows the mechanical frame of the testing apparatus with its main components. Rubber dampers were used to imitate muscles. Two pneumatic cylinders were responsible for moving and loading. These two pneumatic cylinders had one distance gauges each, and the force applied by the cylinders could be changed to a force of 500 N on one side and only 200 N on the other side. The testing apparatus contained four force gauge cells.

Test programme was developed to be able to run both static and dynamic load cases. In case of static loading, the applied force was set continuous and constant on the structure. Then we examined the displacements that resulted from the force, and how much did the applied force change in the meanwhile. In case of dynamic loading, we were able to set different force magnitudes for different number of cycles: for the first cycle, one side was loaded with 100 N for 2 seconds and the other side was loaded with 400 N, which was then repeated 10 times. In the meanwhile, for example, the apparatus logged

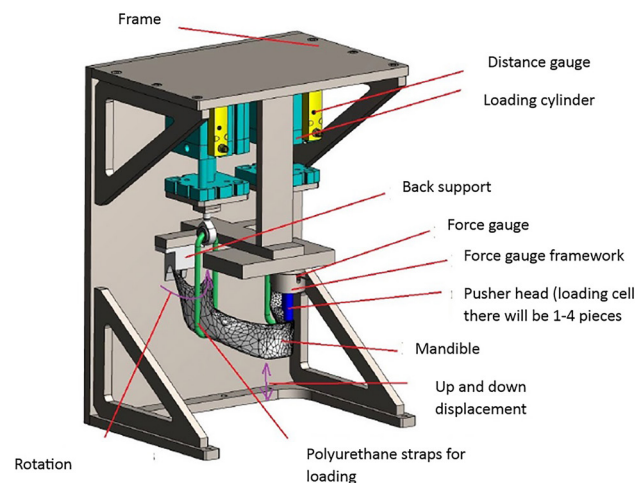


Fig. 1 Mechanical model of the testing apparatus



Fig. 2 Testing apparatus

the results in every fifth loading cycle. The software can save the most important data, for example, magnitude of the loading force, force of proportional valves, force with which we try to move the cylinders, also we could measure the position of the two distance gauges under loading and we could log the measured forces from the four force gauges. PLC enabled saving the data to an Excel table, from which diagrams could be created. The built testing apparatus is shown in Fig. 2. The testing apparatus was submitted for patenting with number: P2300326.

Different implants were tested, which are shown in Fig. 3. Jawbones were created from distinct materials. Material of the first one was Magna Dental Model, then Ultracur3D Photocentric EPD 4006. The third material was Tough 2000 Resin. Printed jawbones from the first two materials and additively manufactured Ti-6Al-4V titanium implants were provided by Dent-Art-Technik Kft. and Premet Kft.



Fig. 3 Printed jaw and titanium implants

### 3 Testing and results

We were able to perform two types of testing on the apparatus, one was static mechanical testing the other was dynamic testing. Fig. 4 shows the position of the abutment on the implant. During calculations, F1 was defined as the real acting force on the back left abutment, F2 was defined as the force acting on the front left abutment, F3 was defined as the force acting on the back right abutment, F4 was defined as the force acting on the front right abutment.

Biting time was selected and constant force was applied by the apparatus for static testing. It is shown in Table 1.

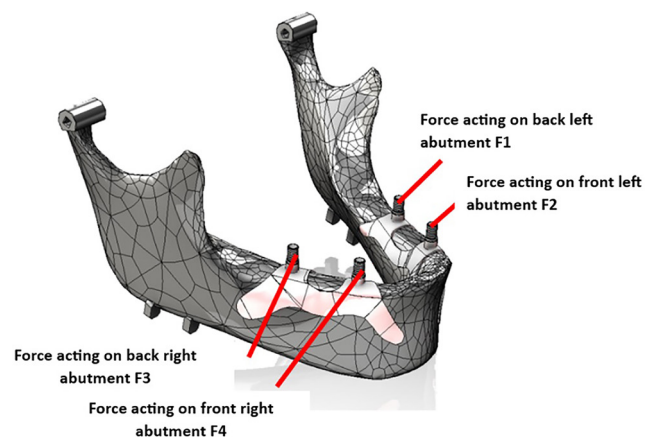


Fig. 4 Position of abutments on the implant

**Table 1** Static parameters

Parameter	1 <sup>st</sup> test	2 <sup>nd</sup> test	3 <sup>rd</sup> test
Right-side loading force [N]	400	100	600
Left-side loading force [N]	600	500	200
Biting time [s]	40	120	180

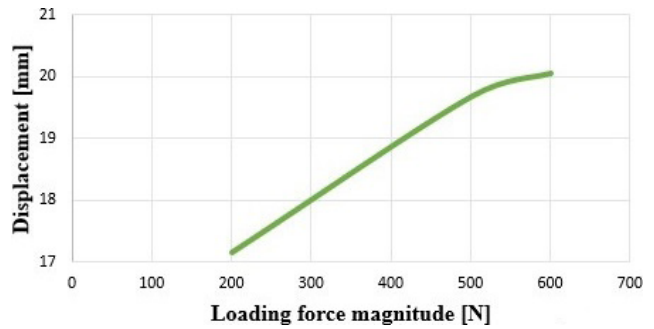
The loading forces were defined to have different magnitudes of forces on the two sides of the jaw. Movement of the jaw was analysed, which meant logging displacement on both the left and right side, and logging forces on different positions (F1, F2, F3, F4). Literature studies show that the jaw must take on most of the forces during chewing. This measurement enables us to define the remaining force on the abutment. Results of static loading are shown in Table 2. During the testing, we encountered the problem that if there are minimal differences in the height of the abutments during production, the pressure stamp only reaches the higher part of the abutment, which is why the first tests produced remarkably small forces, for example the F4 force in the case of the 2<sup>nd</sup> test.

Fig. 5 Shows the magnitude of displacements for both the left and right jaw. It is visible that both sides have the same tendency.

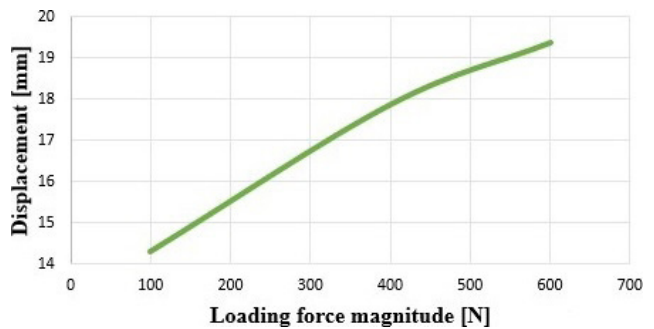
Fig. 6 shows the forces acting on the four abutments. The first case, where the right and left forces were 400 N and 600 N respectively, showed that chewing took place at the frontal part of the mandible. This was the result of the design, as the first two abutments were located above their counterparts in the back. The back left abutment took 31.37% of the loading force, the remaining 68.63% was taken up by the mandible due to the anatomy of chewing. On the right side, the abutment took 21.66% of the total force (78.34% was taken up by the mandible). During the second testing, where the right and left forces were 100 N and 500 N respectively, chewing function was only taken on by the front left abutment: it took 33.68% of the force acting on it. In the third test, where the right and left forces were 600 N and 200 N respectively, the front right abutment took on the chewing function by taking 40.4% of the force acting on it. The next phase of the analysis was dynamic testing. Size and length

**Table 2** Results of static loading

Tests	Left displacement [mm]	F <sub>1</sub> force [N]	F <sub>2</sub> force [N]	Right displacement [mm]	F <sub>3</sub> force [N]	F <sub>4</sub> force [N]
1 <sup>st</sup> test	20.06	1.6	188.2	17.87	0.23	86.64
2 <sup>nd</sup> test	19.68	1.02	168.42	14.31	0.3	0.23
3 <sup>rd</sup> test	17.16	0.15	0.41	19.37	0.34	242.38



(a)



(b)

**Fig. 5** (a) diagram of left-side displacements; (b) diagram of right-side displacements

of pusher heads were identical. There is currently a difference of a few millimetres between the heights of the abutments placed on the implant, so the loading force acted on the right front abutment. Parameters of the four-cycle experiment are shown in Table 3. Table 4 shows the results of the first dynamic test. 600 N of force was applied, but only forces between 191.76 N and 215.56 N were acting on the abutments, which meant 31.96% and 35.93% of the loading force respectively, the rest of the force arose in the jaw. In the second cycle, 500 N of force was applied, and only forces between 156.78 N and 162.21 N were acting on the abutments, which meant 31.36% and 32.44% of the loading force. In the third cycle, 400 N of force was applied, and only force between 128.79 N and 154.79 N were acting on the abutments, which meant 32.19% and 38.7% of the loading force respectively. In the fourth cycle, 300 N of force was applied, and only force between 130.38 N and 135.15 N were acting on the abutments, which meant 43.46% and 45.05% of the loading force respectively. The results showed that 30–45% of the applied force was taken up by the implant and the remaining 55–70% was acting on the mandible due to its chewing movement.

The second dynamic testing was carried out with increased loading forces. In this case, the loading cell reached the front left and front right abutments, so forces

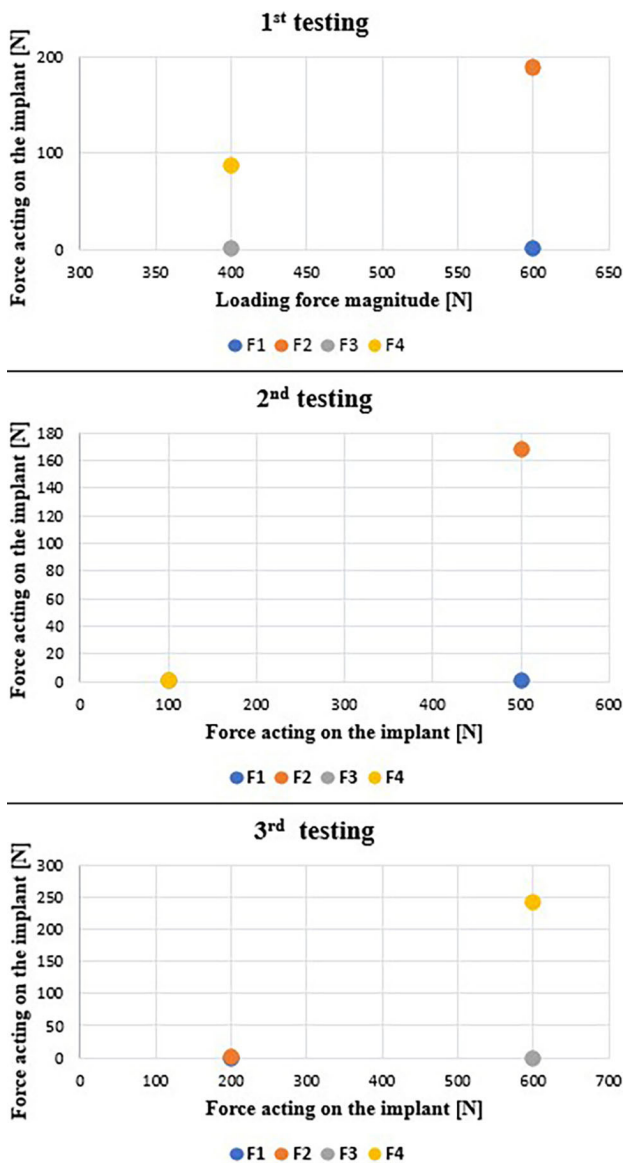


Fig. 6 Magnitude of forces arising in the abutments during each testing

Table 3 Parameters of dynamic loading

Parameters	1 <sup>st</sup> cycle	2 <sup>nd</sup> cycle	3 <sup>rd</sup> cycle	4 <sup>th</sup> cycle
Right-side loading force [N]	600	500	400	300
Left-side loading force [N]	500	100	400	200
Biting time [s]	6	6	15	5
Relaxation time [s]	2	2	2	2
No. of repetitions	10	5	3	15
Sampling in every X part	1	1	1	3

were detected on both of them. The other two abutments did not take up any force as they were lower than the other two. Table 5 shows parameters of testing. Results of dynamic testing are shown in Table 6. In the first cycle, the left-side loading force was 800 N, from which the implant

and the abutment took up 32.37%. The right-side loading force was 600 N, from which the abutment took up 25% on average. In the second cycle, 32.95% of the given loading was taken up on the left side and 46.67% on the right side. In the third cycle, 24.74% of the given loading force was taken up on average on the left side and 33.69% on the right side. In the fourth cycle, average of 38.23% of the loading force was taken up on the left side and 16% on the right side. We could note that if two abutments or superstructures were loaded, 29.16%, 42.47%, 29.21%, and 30.15% were taken up on average from the total force (i.e., adding up both the left and right sides). The results of the first dynamic test presented above were between 30–45%, now it was between 29–43%. Therefore, if the loading force is divided into two parts i.e., on two sides, the force acting on the implant is reduced to a small extent.

#### 4 Results of finite element analysis

We performed static tests using finite element analysis. Finite element analysis is not capable of cyclic dynamic testing as there are no such material properties that make modelling possible. Static testing however, can be carried out. Model of the testing apparatus was used for analysis. We tried to replicate the real-life movements of the testing apparatus during finite element analysis. Perfect models, ideal connections and precision were required for testing. It took a lot of time with the preparations until each piece had an exact fit, because we were able to produce the different pieces with different software. After meshing, boundary conditions followed, making sure to implement the motion of the real testing apparatus. Fig. 7 shows the fixation of the mandible tip, where both X and Y directions were fixed and only rotation was allowed.

On the real testing apparatus, we fixed the lower jaw with a strap, which we can only substitute in finite element analysis, we inserted springs in place, which can be seen in Fig. 8.

The force input takes place on the upper surface of the sleeves (4 sleeves). In this way, they can move in all directions, thus we can ensure the displacements resulting from the chewing function. Fig. 9 shows the meshing of the jaw and the implant. The vertex number: 210,678, the element number: 263,934. The jaw was meshed with first-order elements to reduce the model size. At the contact force, it was implemented with 2–3 rows of contacting elements and second-order elements.

During the calculations, we obtain the values that the implant momentarily experiences when the

**Table 4** Results of dynamic testing

Tests	Left displacement [mm]	F <sub>1</sub> force [N]	F <sub>2</sub> force [N]	Right displacement [mm]	F <sub>3</sub> force [N]	F <sub>4</sub> force [N]
1 <sup>st</sup> cycle	14.73	0.2	0.83	19.05	0.7	216.17
	14.77	0.2	0.9	19.13	0.74	215.56
	14.79	0.2	0.86	19.19	0.74	212.01
	14.80	0.24	0.86	19.20	0.74	206.77
	14.81	0.17	0.9	19.22	0.7	202.86
	14.80	0.2	0.86	19.23	0.74	199.86
	14.82	0.2	0.9	19.26	0.7	198.7
	14.82	0.2	0.9	19.3	0.74	196.7
	14.80	0.17	0.86	19.28	0.74	191.83
	14.81	0.2	0.9	19.3	0.74	191.76
2 <sup>nd</sup> cycle	14.83	0.2	0.93	18.72	0.77	162.21
	14.83	0.24	0.93	18.72	0.74	161.19
	14.88	0.2	0.97	18.73	0.77	157.83
	14.88	0.2	0.97	18.71	0.81	156.78
	14.88	0.24	0.9	18.74	0.85	156.85
	18.79	0.39	0.94	17.99	0.77	128.79
3 <sup>rd</sup> cycle	18.83	0.64	0.91	18.03	0.88	145.43
	18.82	0.49	0.91	18.02	0.81	154.79
	17.01	0.28	0.25	17.19	0.81	134.29
4 <sup>th</sup> cycle	16.99	0.28	0.24	17.17	0.77	134.10
	16.94	0.42	0.21	17.12	0.85	135.15
	16.93	0.24	0.23	17.11	0.81	132.48
	16.93	0.42	0.24	17.10	0.92	130.38

**Table 5** Parameters of dynamic testing

Parameter	Number of cycles			
	1 <sup>st</sup> cycle	2 <sup>nd</sup> cycle	3 <sup>rd</sup> cycle	4 <sup>th</sup> cycle
Right-side loading force [N]	600	500	600	400
Left-side loading force [N]	800	200	600	700
Biting time [s]	60	120	150	60
Relaxation time [s]	1	2	1	1
No. of repetitions	10	5	5	10
Sampling in every X part	2	1	1	2

loading force is applied. Parameters of static testing are shown in Table 7. Fig. 10 Shows the test area and pressing surfaces. Magnitude of vertical displacement of the pressing surface in the moment of applying the loading force are shown in Table 8. Fig. 11 shows vertical displacements of the pressing area. Finite element analysis showed the method of perfect displacement. Larger forces

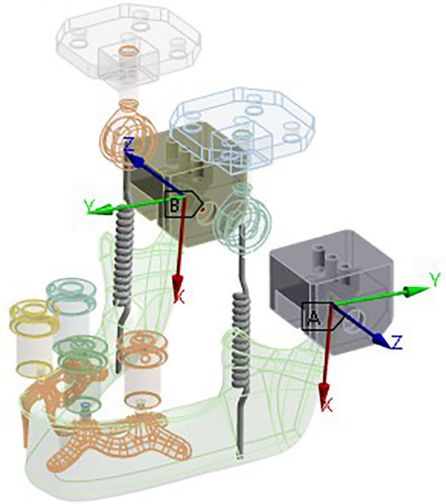
resulted in larger displacements compared to smaller forces. Frontal abutments showed larger displacements in all cases, which corresponded with real-life movements. These results are shown in Fig. 12. Forces were also evaluated at the connection of the implant and abutments. Points of application of forces are shown in Fig. 13. As previously mentioned above, screw force was also calculated here. These are results arising from pressing force. These results also showed perfect connection as loading forces from each pressing head reached the abutments. Thus, it is impossible to correct those errors that arose during real-life testing. Table 9 shows forces acting on the abutments right in the moment of applying the under static loading condition.

Fig. 14 shows the results of the first testing. 59.85% of the loading force acted on the back right abutment, and 66.3% of the loading force acted on the front right abutment. 53.33% of the loading force acted on the back left abutment, while 56.05% acted on the front left abutment. It is shown that momentary contact forces reached values between 53 and 67%, so the environment i.e., the mandible, only took up 33 to 47%. Results of the second test

**Table 6** Results of dynamic testing

Tests	Left displacement [mm]	F <sub>1</sub> force [N]	F <sub>2</sub> force [N]	Right displacement [mm]	F <sub>3</sub> force [N]	F <sub>4</sub> force [N]
1 <sup>st</sup> cycle	21.4	0.92	282.36	19.5	0.32	147.94
	21.56	2.14	254.51	19.66	0.5	152.79
	21.67	2.76	243.19	19.75	0.54	151.99
	21.67	2.47	251.22	19.84	0.68	149.17
	21.85	2.14	259.64	19.9	0.79	148.09
2 <sup>nd</sup> cycle	18.25	0.37	62.29	19.21	0.87	240.46
	17.87	0.41	70.93	19.17	1.01	232.11
	17.81	0.41	62.85	19.18	1.05	229.29
	17.73	0.48	65.14	19.22	1.15	228.13
	17.72	0.52	68.32	19.22	1.26	226.94
3 <sup>rd</sup> cycle	20.78	2.65	143.76	19.88	1.37	209.47
	20.92	2.65	144.64	19.94	1.48	203.53
	20.96	2.58	146.94	19.95	1.55	203.1
	21.01	2.47	150.52	20	1.59	198.33
	21.05	2.4	150.6	20.02	1.81	196.19
4 <sup>th</sup> cycle	21.44	2.25	262.75	18.96	1.81	68.66
	21.48	2.22	270.89	18.91	1.88	64.54
	21.51	2.14	271.94	18.93	1.95	62.19
	51.54	2.07	267.17	18.93	2.02	63.09
	51.54	2.14	265.39	18.92	2.06	61.61

- A** Revolute - 2022-002-000-01-A\_Holder\Solid1 To SYS-2\Patch body
- B** Revolute - 2022-002-000-01-A\_Holder\Solid1 To SYS-2\Patch body



**Fig. 7** Boundary condition, rotation is permitted along axis "z"

are shown in Fig. 15 49.6% of the loading force acted on the back right abutment, and 58.8% of that acted on the front right abutment. 44.64% of the loading force acted on the back left abutment, and 47.66% of that acted on the front left abutment. It is shown that momentary contact forces resulted in values between 44 and 59%. This

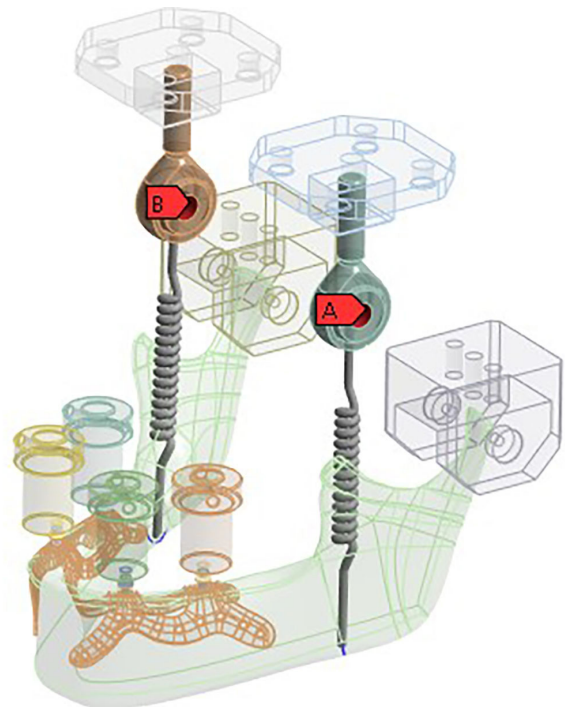


**Fig. 8** Spring stiffness for modelling the straps

meant that the environment i.e., the mandible took up 41 to 56%. Results of the third test are shown in Fig. 16 49.9% of the loading force acted on the back right abutment,

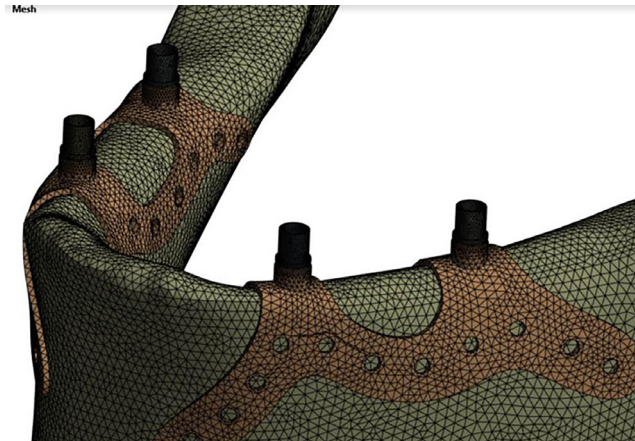


Fig. 9 Meshing of the jaw and the subperiosteal implant

Table 7 Static parameters

Parameters	1 <sup>st</sup> testing	2 <sup>nd</sup> testing	3 <sup>rd</sup> testing
Right-side loading force [N]	400	100	600
Left-side loading force [N]	600	500	200

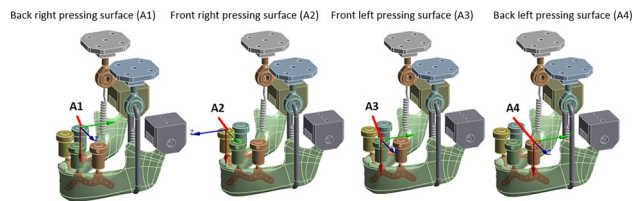


Fig. 10 Locations of the vertical displacement of pressing surfaces

Table 8 Vertical displacement of pressing surfaces

Test	A <sub>1</sub> displacement [mm]	A <sub>2</sub> displacement [mm]	A <sub>3</sub> displacement [mm]	A <sub>4</sub> displacement [mm]
1 <sup>st</sup> test	0.167	0.202	0.208	0.171
2 <sup>nd</sup> test	0.111	0.129	0.137	0.115
3 <sup>rd</sup> test	0.143	0.169	0.164	0.135

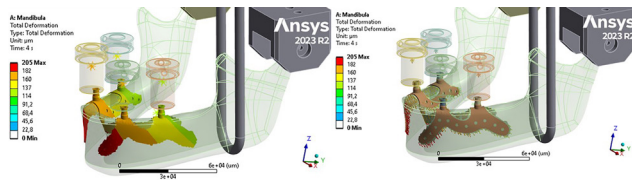


Fig. 11 Displacement of implants and mandible

and 54.27% of that acted on the front right abutment. 66.8% of the loading force acted on the back left abutment, and 62.4% of that acted on the front left abutment. It is shown that momentary contact forces resulted in values between 49 and 67%. This meant that the environment i.e., the mandible took up 37 to 51%.

Weak point of the implant system was located at the connection of sleeve and abutment. The maximum force rises

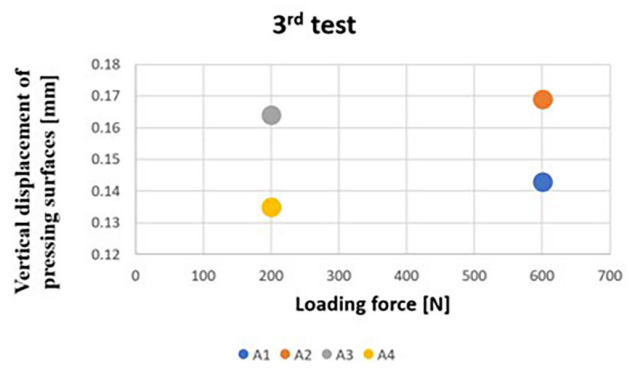
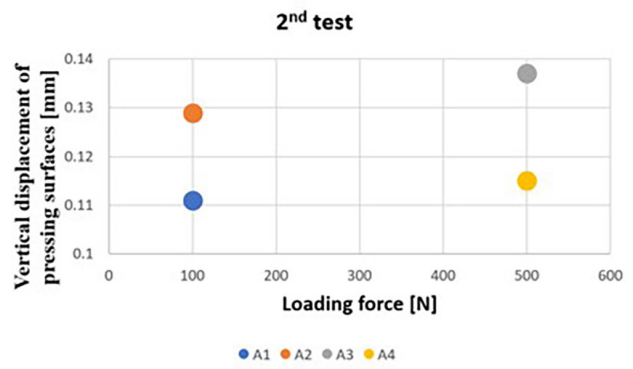
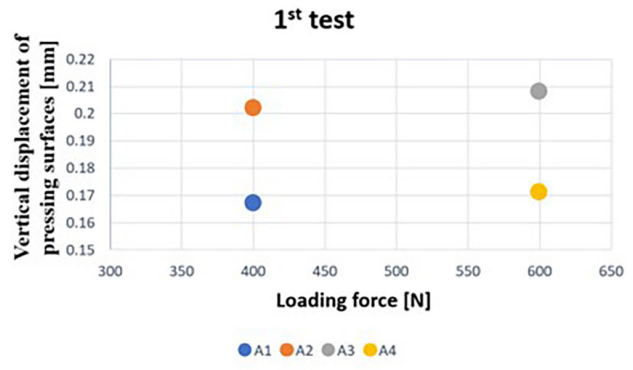


Fig. 12 Vertical displacement of pressing surface

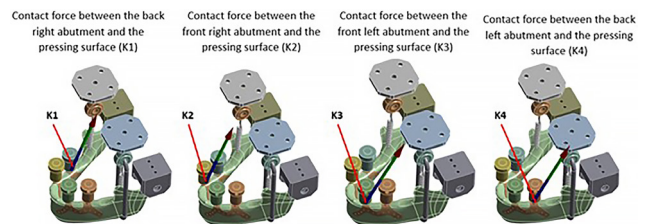


Fig. 13 Locations of contact force arising between the abutments and pressing surfaces

Table 9 Contact force between sleeve and pressing surface

Test	K <sub>1</sub> contact force [N]	K <sub>2</sub> contact force [N]	K <sub>3</sub> contact force [N]	K <sub>4</sub> contact force [N]
1 <sup>st</sup> test	239.4	265.2	336.3	319.6
2 <sup>nd</sup> test	71.5	91.5	238.3	223.2
3 <sup>rd</sup> test	299.4	325.6	124.8	133.6

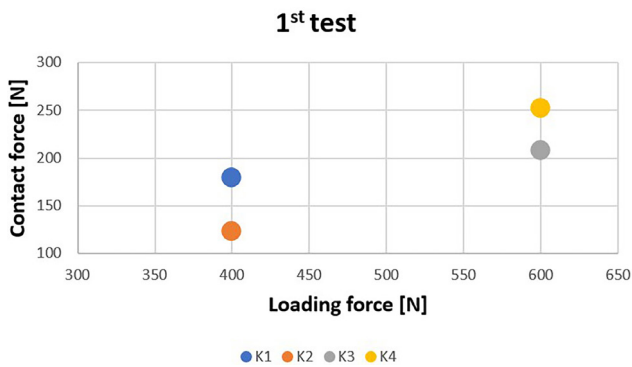


Fig. 14 Results of the first static testing

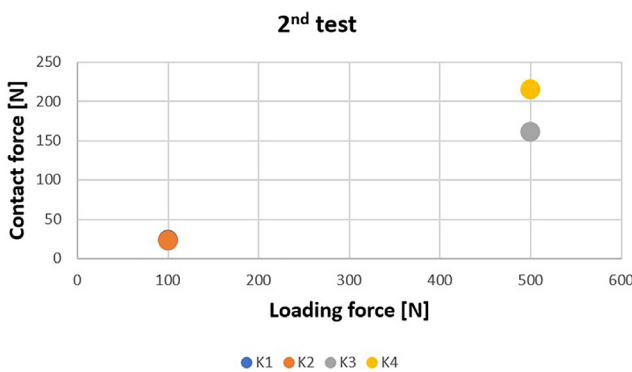


Fig. 15 Results of the second static testing

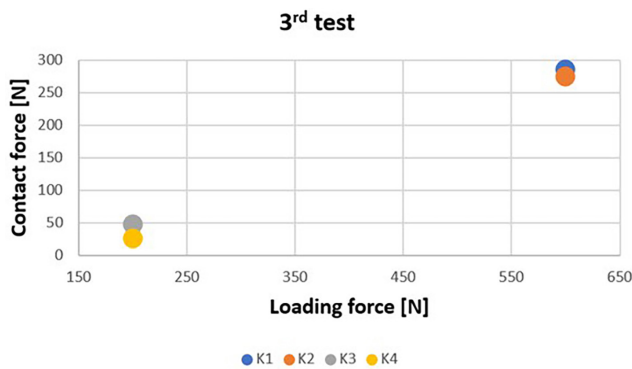


Fig. 16 Results of the third static testing

at the upper border of the sleeve as both pressing force and screw force acted at the same time. Moreover, it acted as a connection surface, but this affected only a limited zone.

### 5 Comparison of real-life tests with theoretical method

Fig. 17 shows the results obtained with the finite element analysis and the testing apparatus. In this case, a load force of 400 N was applied on the right side, while a force of 500 N was applied on the left side.

The Fig. 17 also shows that the results of the finite element analysis and the tests performed on the testing apparatus

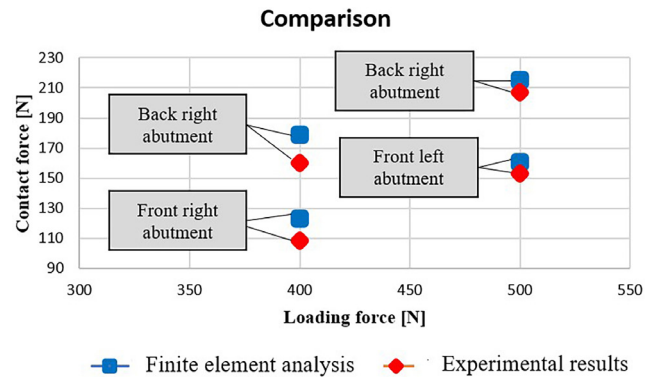


Fig. 17 Comparison of the theoretical and the experimental results

correlate well with each other. With the help of the new testing apparatus and the finite element analysis, it can be determined how much of the real chewing force is taken up by the implant and the jaw. Various production errors and dimensional differences can be eliminated, while this cannot be done with numerical analysis, since finite element analysis requires perfect 3D models and precise connection surfaces, which in reality is not always feasible in production. Both the finite element analysis and the testing apparatus can be used to determine the real force arising from the chewing force on the implant, as well as the extent of the displacements. The advantage of the testing apparatus over the finite element analysis simulation is that after 3D printing, not only static but also dynamic tests can be performed, and manufacturing errors can be eliminated during testing, so with the testing apparatus we get results faster and the deformation on the implant can be easily monitored.

### 6 Conclusion

Novel, custom-made testing apparatus made it possible to mechanically test subperiosteal implants:

It became possible to determine the forces acting between the implant abutments and the mandible that resulted from mechanical loads (chewing forces). It became possible to eliminate manufacturing errors and especially errors caused by different heights of the abutments. It became possible to explore welding and screwing problems. We could not find a suitable solution to these problems with finite element analysis.

### Acknowledgement

The research was supported by the NKFIH from the project 'Research on the health application of artificial intelligence, digital imaging, employment and material technology developments by linking the scientific results of Széchenyi

István University and Semmelweis University' under grant number TKP2021-EGA-2. The authors thank for the support of ActiTOX project funding from the European

Union's Horizon 2020 MSCA-RISE Marie Skłodowska-Curie Research and Innovation Staff Exchange Research Programme under grant agreement no. 823981.

## References

- [1] Kandasamy, S., Greene, C. S., Rinchuse, D. J., Stockstill, J. W. (eds.) "TMD and Orthodontics: A clinical guide for the orthodontist", Springer, 2015. ISBN 978-3-319-19781-4  
<https://doi.org/10.1007/978-3-319-19782-1>
- [2] Koolsrta, J. H. "Dynamics of the human masticatory system", *Critical Reviews in Oral Biology & Medicine*, 13(4), pp. 366–376, 2002.  
<https://doi.org/10.1177/154411130201300406>
- [3] Ahlgren, J., Öwall, B. "Muscular activity and chewing force: A polygraphic study of human mandibular movements", *Archives of Oral Biology*, 15(4), pp. 271–280, 1970.  
[https://doi.org/10.1016/0003-9969\(70\)90053-1](https://doi.org/10.1016/0003-9969(70)90053-1)
- [4] Anusavice, K. J. "Phillips' Science of Dental Materials", Elsevier Health Sciences, 2003. ISBN 9781437725490
- [5] Takanobu, H., Maruyama, T., Takanishi, A., Ohtsuki, K., Ohnishi, M. "Mouth opening and closing training with 6-DOF parallel robot", In: *Proceedings 2000 ICRA. Millennium Conference. IEEE International Conference on Robotics and Automation. Symposia Proceedings (Cat. No.00CH37065)*, San Francisco, CA, USA, 2000, pp. 1384–1389. ISBN 0-7803-5886-4  
<https://doi.org/10.1109/ROBOT.2000.844791>
- [6] Alemzadeh, K., Jones, S. B., Davies, M., West, N. "Development of a Chewing Robot With Built-in Humanoid Jaws to Simulate Mastication to Quantify Robotic Agents Release From Chewing Gums Compared to Human Participants", *IEEE Transactions on Biomedical Engineering*, 68(2), pp. 492–504, 2021.  
<https://doi.org/10.1109/TBME.2020.3005863>
- [7] Wen, H., Cong, M., Zhang, Z., Wang, G., Zhuang, Y. "A Redundantly Actuated Chewing Robot Based on Human Musculoskeletal Biomechanics: Differential Kinematics, Stiffness Analysis, Driving Force Optimization and Experiment", *Machines*, 9(8), 171, 2021.  
<https://doi.org/10.3390/machines9080171>
- [8] Raabe, D., Harrison, A., Ireland, A., Alemzadeh, K., Sandy, J., Dogramadzi, S., Melhuish, C., Burgess, S. "Improved single- and multi-contact life-time testing of dental restorative materials using key characteristics of the human masticatory system and a force/position-controlled robotic dental wear simulator", *Bioinspiration & Biomimetics*, 7(1), 016002, 2012.  
<https://doi.org/10.1088/1748-3182/7/1/016002>
- [9] Negrini, G. "Development of a test protocol for the mechanical analysis of custom-made sub-periosteal dental implants: numerical – experimental integrated approach", MSc Thesis, Politecnico Milano 1863, 2021.
- [10] Altıparmak, N., Polat, S., Onat, S. "Finite element analysis of the biomechanical effects of titanium and Cfr-peek additively manufactured subperiosteal jaw implant (AMSJI) on maxilla", *Journal of Stomatology, Oral and Maxillofacial Surgery*, 124(1), 101290, 2023  
<https://doi.org/10.1016/j.jormas.2022.09.011>
- [11] De Moor, E., Huys, S. E. F., van Lenthe, G. H., Mommaerts, M. Y., Vander Sloten, J. "Mechanical evaluation of a patient-specific additively manufactured subperiosteal jaw implant (AMSJI) using finite-element analysis", *International Journal of Oral and Maxillofacial Surgery*, 51(3), pp. 405–411, 2022.  
<https://doi.org/10.1016/j.ijom.2021.05.011>
- [12] Chang, Y., Tambe, A. A., Maeda, Y., Wada, M., Gonda, T. "Finite element analysis of dental implants with validation: to what extent can we expect the model to predict biological phenomena? A literature review and proposal for classification of a validation process", *International Journal of Implant Dentistry*, 4(1), 7, 2018.  
<https://doi.org/10.1186/s40729-018-0119-5>
- [13] Cepic, L. Z., Frank, M., Reisinger, A. G., Sagl, B., Pahr, D. H., Zechner, W., Schedle, A. "Experimental validation of a micro-CT finite element model of a human cadaveric mandible rehabilitated with short-implant-supported partial dentures", *Journal of the Mechanical Behavior of Biomedical Materials*, 126, 105033, 2022.  
<https://doi.org/10.1016/j.jmbbm.2021.105033>